A Novel Small-Ratio Relative-Rate Technique for Measuring OH Formation Yields from the Reactions of O_3 with Alkenes in the Gas Phase, and Its Application to the Reactions of Ethene and Propene

Suzanne E. Paulson,* Jill D. Fenske,‡ Atish D. Sen, and Tyrone W. Callahan†

Department of Atmospheric Sciences, University of California at Los Angeles, Los Angeles, California 90095-1565

Received: October 23, 1998; In Final Form: January 26, 1999

A small-ratio relative-rate technique to derive OH yields from O_3 reactions with alkenes is described. OH tracer compounds—aromatic and aliphatic hydrocarbons—are added to O_3−alkene mixtures in small quantities. Under these conditions, a large fraction of the tracer is consumed, resulting in a large signal that allows accurate determination of OH formation yields. Analytical approximations, numerical analysis, and sources of random and systematic uncertainties are discussed. This method is applied to measuring the OH formation yield from the O_3 reaction with propene and ethene, finding 0.35 ± 0.07 and 0.18 ± 0.06, respectively.

Introduction

The reactions of ozone with alkenes in the gas phase produce a complex set of stable and radical products (e.g., ref 1). Several recent studies have provided evidence that these reactions lead to the direct production of OH radicals.[2−8] Organic peroxy radicals (RO_2) are likely to accompany the production of OH.[2] OH and RO_2 radical formation from these reactions has a significant impact on the atmospheric chemistry of urban and rural air. In those regions of the atmosphere with moderate alkene concentrations (a few hundred ppt or more), OH and RO_2 formation from O_3−alkene reactions is a major, and sometimes dominant, component of primary HO_x production (HO_x = OH, HO_2, and RO_2) during both day and night.[9,10] In air that is heavily influenced by anthropogenic emissions, the majority of HO_x comes from trace quantities of alkenes with internal double bonds.[9] In rural continental air the major alkene contributors are isoprene and α-pinene, but trace quantities of terpenes with internal double bonds can also be significant.[9]

Five lines of experimental evidence indicate OH is formed in the ozonolysis of alkenes: (1) excess alkene consumption compared to O_3 consumption (indicating an additional loss process for the alkene[2,11]); (2) reaction of tracers that react with OH but only slowly with O_3 (e.g. refs 12 and 13), (3) formation of products that are consistent with reaction of OH with alkenes and tracers (e.g. refs 3, 5, and 13−15); (4) recent studies monitoring relative consumption rates of pairs of tracers are consistent with OH reaction;[6,8] (5) most importantly, Donahue et al.,[7] have very recently observed the OH radical directly using laser induced fluorescence (LIF) in low-pressure flow tube studies of ozone−alkene reactions. The OH formation mechanism involving a vibrationally excited hydroperoxide intermediate (R6) has also recently been thermochemically described.[7,16,17]

The above methods have also been applied to quantify OH yields. A large, self-consistent data set has been developed by Atkinson and co-workers,[3,5,18] by monitoring products from reaction of cyclohexane with OH in O_3−alkene systems. OH reacts with cyclohexane to make an RO_2 radical that disproportionates to cyclohexanone plus cyclohexanol. The RO_2 radicals can also react with HO_2 to form hydroperoxides. Since the HO_2 concentration in the reactor is not known, the cyclohexanone/cyclohexanol method carries an uncertainty of −33%+50%. Tracer loss methods where the tracer is at equal or higher concentration than the alkene, and other methods,[19,20] generally have higher uncertainties. Recently, Atkinson and co-workers have developed a new method that provides OH yield measurements with higher accuracy, about ±15%.[14] This method measures formation of 2-butanone from the reaction of 2-butanol with OH, a reaction that does not involve an RO_2 intermediate. Because the 2-butanol contains small quantities of impurities that result in the formation of 2-butanone in the absence of alkenes, this method is best applied to alkenes that react rapidly with ozone (i.e., $k > 8 \times 10^{-17}$ cm^3 molecule^{-1} s^{-1}). Gutbrod et al.[15−17] have recently measured OH formation by adding CO in large excess and monitoring CO_2 formation. They report OH yields that are in most cases lower than other measurements. The LIF measurements carried out at 4−7 Torr by Donahue et al. have estimated uncertainties of ∼±50%, and since the pressure dependence of OH formation has yet to be established, the quantitative comparability of these measurements is not clear.

In this work, we discuss the theoretical basis of a small-ratio relative-rate technique for measuring OH yields with high precision (±15−25%), and its application to measuring OH formation from propene. The method takes advantage of the behavior of the kinetics when a small quantity of tracer is added, and the majority of OH reacts with the alkene, rather than the tracer. Under these conditions, a large fraction of the tracer is consumed (up to 60%). The method is most successful when the tracers react rapidly with the OH radical, and very slowly with ozone. 1,3,5-Trimethylbenzene (TMB) is an excellent choice, followed by *m*-xylene (XYL) and di-*n*-butyl ether (DBE).

Mechanism of O_3−Alkene Reactions

The reaction of O_3 with alkenes is believed to occur via the formation of a five-membered ring intermediate that decomposes to produce a carbonyl compound and the so-called "Criegee

* Corresponding author. Email: paulson@atmos.ucla.edu
‡ Department of Chemical Engineering.
† Department of Finance.

10.1021/jp984140v CCC: $18.00
Published on Web 03/17/1999

intermediate" (CI) (e.g., ref 21). For ethene:

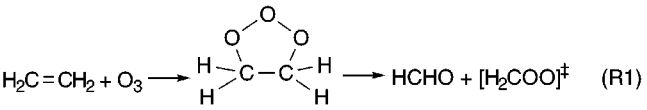

(R1)

Most of the initial CI is vibrationally excited and either decomposes or is collisionally stabilized by the surrounding gas (R2). Ab initio calculations of this reaction suggest that the OH formation channel (R2f) accounts for 5−15% of the total,[7,16] in reasonable agreement with experiments (e.g., ref 5).

$$[H_2COO]^{\ddagger} \xrightarrow{(M)} H_2COO(\text{"thermalized"}) + M \quad (R2a)$$

$$HC(O)OH + M \quad (R2b)$$

$$\rightarrow 2H + CO_2 \quad (R2c)$$

$$H_2O + CO \quad (R2d)$$

$$CO_2 + H_2 \quad (R2e)$$

$$OH + HCO \quad (R2f)$$

OH Formation. OH formation from ethene and larger alkenes is probably best explained with different mechanisms. For ethene, small amounts of OH may arise from path (R2f) plus the side reactions:

$$H + O_3 \rightarrow OH + O_2 \quad (R3)$$

$$HO_2 + O_3 \rightarrow OH + 2O_2 \quad (R4)$$

There is a growing body of evidence that OH is produced directly in high yield from O_3 reactions with larger alkenes, through a different mechanism than that of CH_2OO. OH formation has been postulated to occur via the formation of a vibrationally excited unsaturated hydroperoxide.[2,22] For propene

$$CH_3HC{=}CH_2 + O_3 \rightarrow CH_2O + CH_3CHOO^{\ddagger} \quad (R5a)$$

$$\rightarrow H_2COO^{\ddagger} + CH_3CHO \quad (R5b)$$

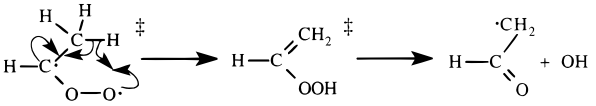

(R6)

Note that since twisting is required for the isomerization; it is not truly concerted. Recent theoretical work suggests that the transition state for the hydroperoxide channel has lower energy than the transition state for the isomerization pathways, which form thermalized CI and other decomposition products but not OH.[7,17]

Experimental Description

All experiments except ET-317 were carried out at 296 ± 2 K in Teflon chambers ranging in size from 100 to 250 L. The chambers were placed in a dark enclosure to eliminate any possible photochemistry. Liquid hydrocarbons were evaporated into a stream of air purified with a zero air generator (Thermo Environmental model 111) as the chamber was filled. Gas-phase hydrocarbons were injected with a gastight syringe. Purchased hydrocarbons (Aldrich) had stated purities of 98% or better and were used as received. Hydrocarbon concentrations were monitored throughout the experiments with a gas chromatograph/flame ionization detector (GC/FID) (Hewlett-Packard 5890), equipped with a 30 m × 1 μm film × 0.32 mm ID DB-1 column (J&W). The GC was calibrated daily with a 20.2 ± 0.4 ppm hexane standard (Scott Specialty Gases). Calibration standards for TMB, DBE, propene, and 1-hexene (all certified to ±2%) were run periodically, and these responses, relative to hexane, were used to determine the concentrations of these compounds. For XYL, a per-carbon response factor calculated from the hexane response was multiplied by the number of carbons; this provides a concentration accurate to within ±4% (provided the compound contains only carbon and hydrogen). For relative measurements, however, we are interested in the repeatability through time and changing sample composition. The repeatability of the GC measurements is better than 0.5% (same sample), but this metric overestimates the precision. Over several hours, an FID can drift by 1% or possibly 2%. As an experiment progresses, small product peaks growing near or under the main peaks in a chromatogram can significantly reduce the precision of the measurement. This can be mitigated by careful examination of the chromatograms and periodic variation of the GC temperature programs. In the absence of coeluting peaks, the precision in the GC/FID measurement of hydrocarbon concentrations is ±1−2%; in some cases the uncertainty can be as high as ±5−7%. An error in an initial concentration is amplified in the resulting slopes (see also eq 7 or 8) by a factor of 2−10 or more; the smaller the amount of tracer consumed in an experiment, the larger the amplification factor. This factor may account for a significant fraction of the observed scatter in our data. Ozone was generated in aliquots by flowing pure O_2 (at 100 S cm^3 min^{-1} for 30−90 s) through a mercury lamp generator (JeLight PS-3000−30), and was monitored by UV absorption (Dasibi 1003-RS).

Thirty to sixty minutes after filling the chamber, the initial hydrocarbon concentrations were determined, typically with four measurements, to establish that the chamber contents were well mixed. Next, a series of O_3 aliquots were added, each immediately following injection of a sample into the GC to allow maximum time for mixing and reaction before the next measurement (15−30 min depending on the GC analysis). Each O_3 injection was followed by manual mixing of the chamber to minimize concentration gradients. Mixing is >90% complete in less than 5 min, but since this is a relative measurement that is essentially independent of the O_3 concentration (see below), mixing is not critical. The total volume of added O_3/O_2 aliquots in a typical experiment was about 0.5 L, but was always less than 1% of the volume of the chamber so that a correction for dilution was unnecessary. Experiments lasted 3−5 h and had average O_3 concentrations (the concentration of each aliquot once it was mixed) of 0.5 ppm or less. Between 55 and 75% of the initial alkene was reacted.

Several experiments using the small-ratio approach have been carried out in different experimental systems to ensure that mixing does not bias results. Experiment ET-317 (Table 1) was carried out at the National Center for Atmospheric Research in Boulder, CO, in a long-path FTIR cell. Briefly, the cell was evacuated, then alkene and tracer were added and the cell was pressurized to 720 ± 10 Torr with synthetic air. After a reference spectrum was acquired, an aliquot of O_3 was prepared and swept into the cell to bring the pressure to 750 ± 5 Torr. All injections were made through an 8-port dispersing injector. After one or two spectra were recorded, the cell was evacuated and the procedure repeated with a different O_3 concentration. Consumptions of alkene and TMB were calculated by differencing the initial spectrum with that after O_3 was added. The results from

TABLE 1: Summary of Initial Conditions, Ratios, and OH Yields

				OH yield			OH yield	
alkene/tracer	expt no.	initial concn (ppm)	T_0/A_0 ratio	complete model	eq 5	S^a	eq 7	eq 11[b]
propene	PT-615	93.4						
1,3,5-TMB		5.77	0.062	0.35	0.31	0.54	0.37	0.36
propene	PT-81	3.03						
1,3,5-TMB		0.222	0.073	0.36	0.31	0.53	0.37	0.36
propene	PT-76	49.4						
1,3,5-TMB		7.09	0.14	0.35	0.30	0.49	0.38	0.35
propene	PT-83	3.36						
1,3,5-TMB		0.645	0.192	0.31	0.29	0.44	0.35	0.34
propene	PT-614	9.83						
1,3,5-TMB		8.92	1.01	0.4[c]	0.39	0.26	0.40[c]	0.41[c]
propene	PT-728	0.387						
1,3,5-TMB		2.40	6.21	0.33[c]	0.51	0.068	0.47[c]	0.52[c]
propene	PD-613	28.0						
DBE		6.04	0.21	0.32	0.27	0.24	0.35	0.34
propene	PTD-719	30.0						
DBE		0.494	0.017	0.35	0.20	0.24	0.29	0.25
TMB		4.63	0.16	0.40	0.35	0.53	0.43	0.39
propene	PTD-77	33.2						
DBE		1.81	0.055	0.33	0.23	0.27	0.34	0.31
1,3,5-TMB		1.86	0.056	0.32	0.26	0.50	0.32	0.31
propene	PDT-726	10.9						
DBE		1.72	0.17	0.34	0.23	0.24	0.33	0.31
1,3,5-TMB		1.79	0.16	0.37	0.26	0.43	0.33	0.32
propene	PXT-117-N	9.20						
XYL		0.317	0.036	0.35	0.28	0.24	0.36	0.375
TMB in nitrogen		0.402	0.045	0.35	0.30	0.55	0.42	0.34
average[c]				0.346	0.28		0.353	0.335
standard deviation (2σ)[c]				0.045	0.08		0.070	0.072
ethene	ET-625	67.1						
propene		0.943						
TMB		4.31	0.064	0.15				
ethene	EXT-919	5.22						
m-xylene		0.935	0.18	0.18	0.12	0.24	0.15	0.16
TMB		0.905	0.17	0.18	0.17	0.53	0.19	0.17
ethene	EDT-918	5.89						
DBE		0.716	0.12	0.17	0.11	0.31	0.18	0.135
TMB		0.956	0.16	0.17	0.18	0.54	0.18	0.18
ethene	ET-911	5.59						
TMB		0.89	0.16	0.19	0.22	0.69	0.24	0.23
ethene	ET-317	93						
TMB		9.3	0.10	0.20	0.21	0.75	0.21	0.23
average[c]				0.18	0.17		0.19	0.18
standard deviation (2σ)[c]				0.03	0.09		0.06	0.08

[a] $S \equiv A_0(T_0 - T_t)/T_0(A_0 - A_t)$; calculated using a linear least-squares regression. [b] Because this equation calculates an OH yield for each data point and is very sensitive to the ratios A/A_0 or T/Tr_0, the initial points have high uncertainties and in some cases widely oscillating values, which converge on a constant value for the later data points (Figure 5). We have arbitrarily averaged the last half of the calculated OH yields for the values reported here. [c] The high ratio experiments PT-614 and PT-728 were not included in the averages.

this experiment, like others carried out in the FTIR cell, are in very good agreement with the chamber/GC/FID measurements using sequential O_3 additions. An additional set of experiments were carried out with the same small-ratio technique in a flow system (Fenske and Paulson, in preparation). In these experiments, mixing is complete in 200 ms to 10 s or less. Again, the flow experiments are in excellent agreement with those performed in the Teflon chamber or with the evacuable FTIR cell.

Theoretical Basis of the Small-Ratio Relative-Rate Method

Monitoring OH formation in ozonolysis reactions is confounded by the rapidity of reactions of alkenes compared to most other compounds. Alkenes react with OH at nearly gas-kinetic rates, most with rate constants in the range $(2.6-36) \times 10^{-11}$ cm^3 molecule^{-1} s^{-1}. If the goal is to scavenge the majority of OH radicals (i.e., >95%) with the tracer, then the tracer must be added in large excess—10−1000-fold depending on the tracer/alkene combination. Under these conditions, even if 100% of the alkene is consumed (and especially if the OH formation yield is significantly less than unity), then a small fraction of the tracer reacts:

$$\mathrm{O_3} + \text{alkene} \xrightarrow{k_{\mathrm{O_3}}} y\mathrm{OH} + y\mathrm{RO_2} + x_1\mathrm{R_2C{=}O} + x_2\mathrm{HO_2} + x_3\text{“thermalized” CI} + \text{other products} \quad \text{(R7)}$$

$$\mathrm{OH} + \text{alkene} \,(+\mathrm{M},\mathrm{O_2}) \xrightarrow{k_{\mathrm{A}}} \mathrm{RO_2}\,(+\mathrm{M}) \quad \text{(R8)}$$

$$\mathrm{OH} + \text{tracer} \,(+\mathrm{O_2}) \xrightarrow{k_{\mathrm{T}}} \mathrm{RO_2}\,(+\text{other products}) \quad \text{(R9)}$$

Deriving information from decay of the tracer under these conditions carries a large uncertainty since it requires measuring small differences between large numbers. However, when a

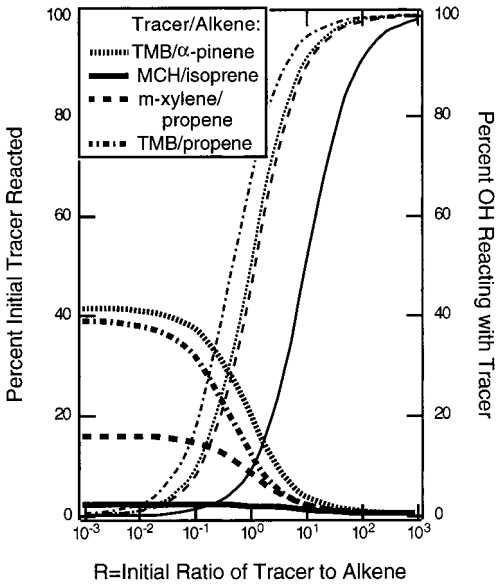

Figure 1. Plot of (a) the percent OH reacting with tracer (thin lines, right axis) and (b) the percent of the initial tracer reacted assuming that 70% of the alkene has reacted in the given experiment (thick lines, left axis). For these calculations, the assumed OH yields were 0.25, 0.35, and 0.7 for isoprene, propene, and α-pinene, respectively. Percents of initial tracer reacted were calculated with eq E7. The rate constants for OH reaction are ($\times 10^{-11}$ cm^3 molecule^{-1} s^{-1}): isoprene, 10; methylcyclohexane (MCH), 1.0; propene, 2.6; 1,3,5-trimethylbenzene (TMB), 5.73; α-pinene, 5.4; and *m*-xylene (XYL), 2.2.

small amount of tracer is added, a measurable percentage of the tracer reacts away.

A tracer can be any compound that reacts rapidly with OH but only slowly with O_3 (or HO_2 or other potential reaction partners). Figure 1 shows the percent OH reacting with tracer (thin lines) and the percent of the initial tracer reacted (thick lines) as a function of the ratio of the initial tracer to alkene concentrations (T_0/A_0), assuming that 70% of the initial alkene has reacted, calculated using eq E7. Three "tracers" are compared: 1,3,5-trimethylbenzene (TMB), *m*-xylene (XYL), and the relatively slowly reacting methylcyclohexane (MCH). These compounds have OH reaction rate constants in the ratio 5.7:2.2:1. As expected, the faster the OH reaction with tracer relative to alkene, the more tracer reacts, at any ratio. This is illustrated by comparing the curves for XYL/propene and TMB/propene; at small ratios, about 2.5 times more TMB is consumed than XYL, in direct proportion to the ratio of their OH rate constants. The MCH/isoprene combination illustrates a particularly poor choice of tracer—isoprene reacts very rapidly with OH, and has a small OH yield, and MCH reacts relatively slowly with OH. These factors combine so that even at very small T_0/A_0 ratios only a few percent of the MCH is consumed. This combination was used by Paulson et al.;[19] the OH yield reported for isoprene in that work should have had a much higher uncertainty estimate. Even with the most rapidly reacting tracer, TMB, a maximum of about 12% is consumed in the isoprene system (not shown). In contrast, for α-pinene, the maximum tracer consumed is about 40% due to more favorable reaction rates and a higher yield of OH from the α-pinene reaction with O_3. Even so, only slightly more tracer reacts in the α-pinene than the propene system (OH yields of 0.7 and 0.35, respectively), because α-pinene competes for OH much more effectively than does propene. It is also apparent that as T_0/A_0 is decreased, the percent of tracer consumed increases, asymptotically approaching a maximum value.

Analytical Approximations of the Small-Ratio Relative-Rate Technique. Because of the changing tracer to alkene ratio, formation of products that also compete for OH, and minor side reactions such as tracer wall losses, the analysis of this type of experiment is done most thoroughly numerically, by solving the differential equations that describe the complete set of reactions in the system (below). A detailed discussion of alternate reactions that may produce small amounts of OH or consume additional tracer appears in the section entitled Systematic Uncertainties.

Two analytical approximations of the kinetics of this method are presented here. The first is intended to provide an intuitive background, and is based only on eqs R7−R9. The second approximation partly compensates for the effect of products from the alkene which also react rapidly with OH and can be applied in special cases.

Analytical Approximation I. The time-dependent concentrations of alkene, tracer, and the OH radical (A, T, and OH, respectively) are given by (based on eqs R7−R9 only):

$$dA/dt = -A(k_A OH + k_{O_3} O_3) \tag{E1}$$

$$dT/dt = -k_T OHT \tag{E2}$$

$$dOH/dt = -OH(k_T T + k_A A) + k_{O_3} O_3 Ay \tag{E3}$$

If OH is assumed to be in steady state, these equations can be rearranged to give the expression:

$$\frac{d \ln T}{d \ln A} = \frac{k_T Ay}{k_A Ay + k_T T + k_A A} \tag{E4}$$

This differential expression must be integrated before an OH yield can be calculated. Use of an integrating factor provides the following expression:

$$A = \frac{T}{y\left(1 - \frac{k_A}{k_T}\right) - \frac{k_A}{k_T}} + \left[A_0 - \frac{T_0}{y\left(1 - \frac{k_A}{k_T}\right) - \frac{k_A}{k_T}}\right]\left(\frac{T}{T_0}\right)^{(k_A/k_T)(y+1/y)} \tag{E5}$$

Unfortunately, (E5) cannot be rearranged to provide a convenient explicit expression for *y*, the OH formation yield, but it can be solved numerically. OH yields from eq E5 were calculated by minimizing the sum of differences between the data and eq E5, are listed in Table 1, and are discussed below.

At small conversions, the *differential* expression (E4) is approximately equal to the slope of a percent tracer reacted vs percent alkene reacted plot (Figures 2−5):

$$\frac{d \ln T}{d \ln A} \approx \frac{A_0(T_0 - T_t)}{T_0(A_0 - A_t)} = S \tag{E6}$$

Thus (E4) and (E6) may be combined to calculate an OH yield:

$$y = \frac{S(k_T T_0 + k_A A_0)}{k_T A_0 - S k_A A_0} \tag{E7}$$

The OH yields calculated with (E7) are included in Table 1. For these calculations a linear least-squares regression was used to calculate the slope for the whole data set, an approach that

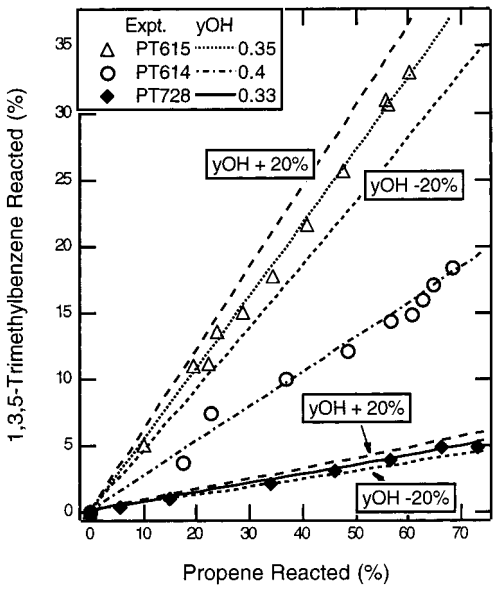

Figure 2. 1,3,5-Trimethylbenzene reacted vs propene reacted for experiments PT-615, -614, and -728 with $T_0/A_0 = 0.062$, 1.01, and 6.21 (Table 1). The symbols represent measurements, and lines model calculations assuming the OH yield specified in the legend. Also shown are the results of calculations assuming a 20% increase or decrease in the OH yield for the small (PT-615) and large (PT-728) ratio experiments. For PT-615, OH yields of 0.42 and 0.28 and for PT-728 0.4 and 0.26 were assumed for the +20% and −20% cases, respectively.

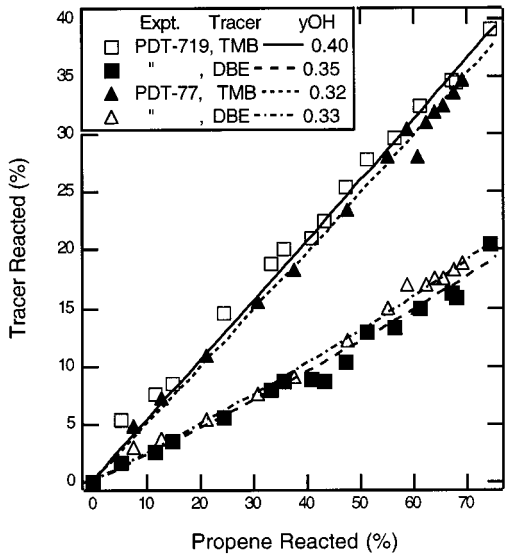

Figure 3. Data (symbols) and calculations (lines) for experiments PDT-77 and PDT-719. The initial ratios for these experiments were and 0.16 and 0.055 for DBE and 0.056 and 0.017 for TMB for experiments PDT-77 and PDT-719, respectively.

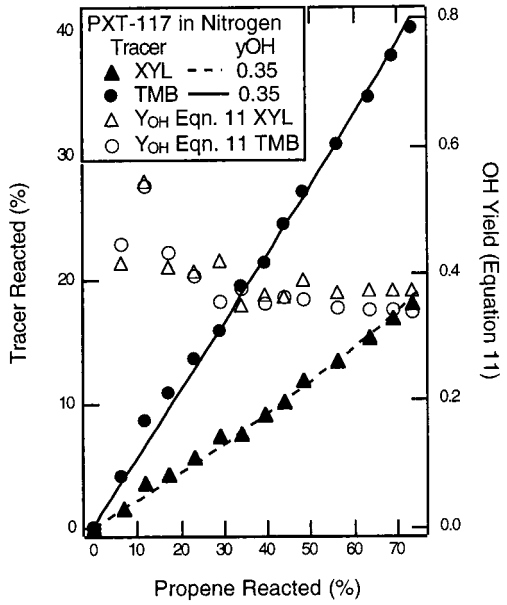

Figure 4. Data (symbols) and calculations with the complete model (lines) for PXT-117-N. Solid circles/solid line are TMB and solid diamonds/dashed line are XYL. An OH yield of 0.35 was assumed for both tracers (Table 1). The open symbols, plotted with respect to the right-hand axis, show the OH yield calculated using eq E11 for each data point; circles for TMB and triangles for XYL.

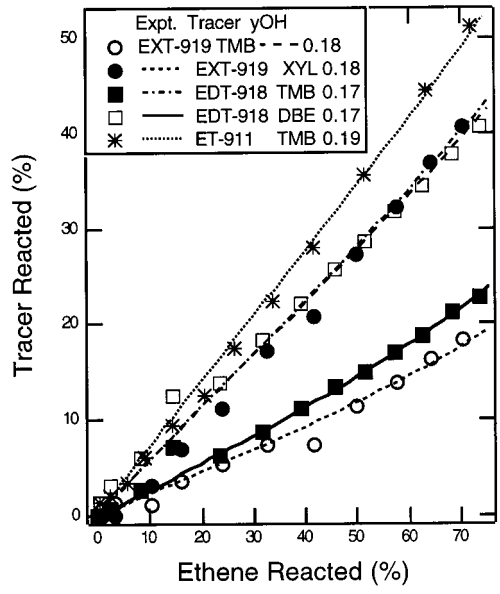

Figure 5. Data (symbols) and calculations (lines) for EXT-919 (circles), EDT-918 (squares), and ET-911 (stars). Corresponding model calculations are indicated in the legend. OH yields of 0.18, 0.17, and 0.19 were assumed for each experiment, respectively (Table 1).

is not strictly correct but works reasonably well for alkenes that produce data that fall on straight lines (discussed below).

Also, when $T_0k_T \ll A_0k_A$,

$$y = \frac{Sk_A}{k_T - Sk_A} \qquad \text{(E8)}$$

Equation E8 is independent of T_0; i.e., the slope (S) of a plot of percent tracer reacted plotted against percent alkene reacted approaches (asymptotically) a maximum value as T_0/A_0 becomes small (Figure 1).

Figure 2 shows data from three TMB/propene experiments, PT-615, -614, and -728, with T_0/A_0 ratios of 0.061, 1.01, and 6.21, respectively (Table 1), plotted as the percent tracer reacted vs percent alkene reacted. As expected, the smaller T_0/A_0, the larger the slope. Model calculations (described below) for these experiments are also shown, assuming OH yields of 0.35, 0.4, and 0.33 for the three experiments, respectively, together with calculations assuming 20% above and below the "best fit" OH yields for PT-615 and PT-728. From these curves it is clear that OH yields can only be determined sensitively by monitoring tracer loss at small T_0/A_0 ratios.

Analytical Approximation II: Accounting for Major Product Formation—A Special Case. The most important additional compounds competing for OH are products. Since in these experiments the alkene is in excess, once half or more

of the alkene has reacted, the concentration of its oxidation products can exceed the concentration of both the alkene and the tracer. Many of the products are less reactive than either the alkene or the tracers and have a small affect. The aldehyde products, however, react reasonably rapidly with OH, and thus can compete significantly for OH:

$$\mathrm{RCHO} + \mathrm{OH} \xrightarrow{k_p} \mathrm{H_2O} + \mathrm{RC(=O)OO^\bullet} \qquad \text{(R10)}$$

An exact analytical solution to the system of ODE's describing (R7)−(R10) could not be obtained, but here we make an approximation that applies to alkenes that make sufficiently reactive products that they effectively replace most of the reacted alkene in competing for OH.

The data (and numerical calculations) for propene and ethene shown in Figures 2−5 fall essentially on straight lines. This implied simplicity is fortuitous. For many alkenes, a slight upward curvature in the lines is observed (e.g., see ref 23), while larger *initial* T/A ratios result in smaller slopes (Figure 2); in a given experiment the increasing T/A ratio tends to increase the slope. The degree of curvature is a complex function of rate constants of alkene, tracer and products, T_0/A_0, and the OH and product yields. For some alkenes, the products have sufficient concentration and reactivity to approximately make up for the amount of alkene needed to maintain the *effective* T/A ratio (note that this is less than the amount of alkene reacted since some of the tracer has also reacted). Under these conditions we can make the approximation:

$$\frac{k_T T_0}{k_A A_0} = \frac{k_T T}{k_A A + k_p P} \qquad \text{(E9)}$$

If we make the further simplification of using k_p and P as the weighted average concentrations and OH reaction rate constants of all reactive products and ignore the decay of P, we can rewrite (E3) as follows:

$$\mathrm{d}OH/\mathrm{d}t = O_3 k_{O_3} y A - OH(k_A A + k_T T + k_p P) \qquad \text{(E10)}$$

(E1), (E2), and (E10) can be integrated to give the following explicit expression for y:

$$y = \frac{\dfrac{(k_T T_0 + k_A A_0)}{(k_T - k_A)}\left(\dfrac{T}{T_0} - \left(\dfrac{T}{T_0}\right)^{(k_A/k_T)}\right)}{A - A_0\left(\dfrac{T}{T_0}\right)^{(k_A/k_T)}} \qquad \text{(E11)}$$

This expression provides a reasonable result for many alkenes, but cannot be used for alkenes that react very rapidly with OH, e.g., isoprene, butadiene, etc., or produce slowly reacting products (e.g., 2,3-dimethyl-2-butene). The results calculated from this expression are also listed in Table 1 and are shown in Figure 4. This equation calculates an OH yield for each data point and is very sensitive to the ratios A/A_0 and T/T_0. Since the measurement error (±1−2%) is similar in magnitude to the percent reacted for the early points, the initial data have high uncertainties that in some cases result in widely oscillating yields calculated with (E11); yields converge to a constant value for the later data points. We have arbitrarily averaged the OH yields calculated from the last half of the data points with (E11) for each experiment to derive the OH yield reported in Table 1, column 9.

Table 1 contains OH yields calculated for each experiment with the complete model and with (E5), (E7), and (E11). The complete model is most reliable since it includes wall losses, product formation, and other minor sources of OH. All three approximations perform poorly for the high ratio experiments, and these have been omitted from the averages. (E5), which accounts for the affects only of (R7)−(R9), results in OH yields that are both smaller and much more variable than those calculated with (E7) or (E11) or with the complete model, averaging 0.28 ± 0.08 for propene and 0.17 ± 0.09 for ethene, compared to 0.35 ± 0.045 and 0.18 ± 0.03 for the model, respectively. The OH yields are particularly low for the more slowly reacting tracer in the dual tracer experiments. Both of these effects arise from other compounds that also react with OH but were ignored in the derivation of (E5): products, and, in the case of the dual tracer experiments, the other tracer. The OH yields calculated from (E5) are somewhat higher for the ethene single-tracer experiments. Ethene is a special case, because it reacts slowly enough with both ozone and OH that the small secondary sources of OH, such as (R4), have a noticeable effect.

Equations E7 and E11 both perform reasonably well, providing average OH yields for the small-ratio experiment that are close to the model results but have much higher scatter. Equation E7 performs well for ethene and propene because they produce data that happens to fall on a straight line, so that the assumption in its derivation, only strictly true at small conversions, gives the appearance of working for the whole experiment. (E11) performs well for propene because the approximation in (E9) is nearly satisfied; the acetaldehyde and formaldehyde formed approximately replace the reacted propene in competing for OH. For ethene, the formaldehyde produced more than replaces the ethene, so (E11) calculates higher OH yields for the single-tracer experiments than does the model. Neither (E7) nor (E11) accounts for a second tracer. For dual tracer experiments, the more slowly reacting tracers generally have lower OH yields than the model for both (E7) and (E11), reflecting the situation that from the point of view of the more slowly reacting tracer the fast reacting tracer consumes a significant fraction of OH, (the reverse is not true).

In summary, several analytical approximations are offered. For a particular experimental design, one or more approximations may work very well, but each must be applied after careful consideration of the particular experiment. That (E7) and (E11) provide results that are very close to the complete model indicates that these experiments are well described by reactions R7−R10. Wall effects and other side reactions have a minor effect.

Numerical Derivation of the OH Yield

While the approximate analytical solutions ((E7) and (E11)) provide reasonable estimates of the OH yield for many alkenes, they do not account for some second-order affects or experiments in which two tracers are used. A kinetics model, solved numerically,[24] that includes organic and inorganic chemistry (shown in Table 2) provides a more accurate OH yield (although for some alkenes the result from (E7) or (E11) is indistinguishable) and provides a way to assess uncertainties. In this calculation, the OH yield from the O_3−alkene reaction is the only parameter adjusted to fit the results. The 47-reaction model we used accounts for the most important reactions, but many products can be safely ignored or lumped. Many of the stable products are relatively unimportant since their concentrations are small until late in the experiment, and they react relatively slowly with OH and not at all with O_3. Tracer product concentrations are always low since the tracer concentrations

TABLE 2: Table of Kinetic Data Used in Model

rate constant at 298 K	ref (k)	ref (products)	reaction and products
(1) 2.63E−11	*a*	*a*	propene + OH → 0.66 2°-β-hydroxy-RO_2 + 0.33 1°-β-hydroxy-RO_2
(2) 1.1E−17	*a*	*b*	propene + O_3 → 0.6formaldehyde + 0.52acetaldehyde + 0.12HO_2 + 0.17CO + 0.25 1°-β-hydroxy-RO_2 + 0.35OH
(3) 1.4E−11	*c*	*a*	acetaldehyde + OH → CH_3CO_3
(4) 3.E−12	*a*	*a*	$CH_3CH_2C(=O)OO$ + HO_2 → $CH_3C(=O)OOH$
(5) 3.E−12	*d*	*d*	CH_3CO_3 + HO_2 → $CH_3C(=O)OOH$
(6) 1.66E−11	*d*	*d*	CH_3CO_3 + CH_3CO_3 → 2.0CH_3OO
(7) 3.7E−13	*d*	*d*	CH_3OO + CH_3OO → 0.72HO_2 + 0.07ROOH + 1.29formaldehyde + 0.57alcohol
(8) 5.8E−12	*d*	*d*	CH_3OO + HO_2 → methylhydroperoxide
(9) 2.1E−12	*d*	*d*[1]	1°-β-hydroxy-RO_2 + 1°-β-hydroxy-RO_2 → formaldehyde + acetaldehyde + HO_2 + 0.5alcohol + 0.5propanal[j]
(10) 1.5E−11	*d*	*d*	1°-β-hydroxy-RO_2 + HO_2 → ROOH
(11) 8.4E−13	*d*	*d*	2°-β-hydroxy-RO_2 + 2°-β-hydroxy-RO_2 → 1.16acetaldehyde + 1.16formaldehyde + 1.16HO_2 + 0.42alcohol + 0.42acetone[j]
(12) 1.5E−11	*d*	*d*	2°-β-hydroxy-RO_2 + HO_2 → ROOH
(13) 1.7E−12	*d*	*d*	1°-β-hydroxy-RO_2 + 2°-β-hydroxy-RO_2 → 0.54acetaldehyde + 1.62formaldehyde + 1.08HO_2 + 0.46alcohol + 0.46acetone[j]
(14) 2.E−11	*a*	*a*	propanal + OH → $CH_3CH_2C(=O)OO$
(15) 5.3E−12	*a*	*a*	OH + alcohol → HO_2 + formaldehyde
(16) 5.5 E−12	*a*	*a*	OH + methylhydroperoxide → 0.67CH_3OO + 0.33formaldehyde[j] + 0.33OH
(17) 5.5 E−12	*a*	*a*	OH + $CH_3C(=O)OOH$ → 0.67CH_3CO_3 + 0.33formaldehyde + 0.33OH
(18) 1.0E−11	*c*	*c*	formaldehyde + OH → HO_2 + CO + H_2O
(19) 5.0E−14	*c*	*c*	formaldehyde + HO_2 → $HOCH_2O_2$
(20) 153	*a*	*a*	$HOCH_2O_2$ → HO_2 + formaldehyde
(21) 6.8E−14	*c*	*c*	OH + O_3 → HO_2 + O_2
(22) 2.E−15	*c*	*c*	HO_2 + O_3 → OH + 2O_2
(23) 1.7E−12	*c*	*c*	HO_2 + HO_2 → HOOH + O_2
(24) 4.9E−32	*c*	*c*	HO_2 + HO_2 + M → HOOH + O_2
(25) 1.7E−12	*c*	*c*	HOOH + OH → HO_2 + H_2O
(26) 1.1E−10	*c*	*c*	OH + HO_2 → H_2O + O_2
(27) 2.8E−11	*d*	*f*	di-*n*-butyl ether + OH → RO_2
(28) 1.E−21	*g*	*f*	di-*n*-butyl ether + O_3 → RO_2
(29) 1.7E−7	*g*	*f*	di-*n*-butyl ether → M (wall loss)
(30) 2.20E−11	*g*	*h*	*m*-xylene + OH → 0.21formaldehyde + 0.89formic acid + 0.33acetic acid[j] + 0.48glyoxal[j] + 0.24 4-oxo-2-methyl-2-pentenal[j] + 0.12 3,5-dimethyl benzaldehyde[j] + 0.152,4,6-trimethyl phenol[j]
(31) 1.E−21	*e*	*f*	*m*-xylene + O_3 → RO_2
(32) 1.6E−7	*e*	*f*	*m*-xylene → M (wall loss)
(33) 5.73E−11	*e*	*h*	TMB + OH → 0.21formaldehyde + 0.89formic acid + 0.33acetic acid + 0.48glyoxal + 0.24 4-oxo-2-methyl-2-pentenal + 0.13 2,5-dimethylbenzaldehyde + 0.15 2,4,6-trimethylphenol
(34) 2.3E−21	*e*	*f*	TMB + O_3 → RO_2
(35) 9.6E−7	*e*	*f*	TMB → M (wall loss)
(36) 3.E−13	*d*	*d*	RO_2 + RO_2 → 2.0RALD + 1.2HO_2
(37) 3.E−12	*d*	*d*	RO_2 + HO_2 → ROOH
(38) 1.E−11	*f*	*f*	ROOH + OH → RALD + OH + RO_2
(39) 3.04E−11	*f*	*f*	RALD + OH → RO_2
(40) 8.E−13	*a*	*a*	acetic acid + OH → CH_3OO
(41) 6.15E−12	*f*	*f*	RACID + OH → 0.12 CO + RO_2
(42) 2.7E−10	*i*	*f*	4-oxo-2-methyl-2-pentenal + OH → RO_2
(43) 4.E−18	*i*	*f*	4-oxo-2-methyl-2-pentenal + O_3 → RO_2
(44) 3.E−11	*i*	*h*	2,4,6-trimethyl phenol + OH → 0.21formaldehyde + 0.89formic acid + 0.33acetic acid + 0.35glyoxal phenol[j] + 0.13methyl glyoxal[j] + 0.24 4-oxo-2-methyl-2-pentenal[j] + 0.12 3,5-dimethyl benzaldehyde[j] + 0.15 2,4,6-trimethyl
(45) 1.12E−11	*i*	*f*	glyoxal + OH → 0.6OH + 0.4CH_3CO_3
(46) 1.8E−11	*i*	*f*	3,5-dimethylbenzaldehyde + OH → RO_2
(47) 4.E−9	*f*	*f*	M = O_3 (artificial O_3 source)

[a] Reference 28. [b] Based on the carbonyl yields of Grosjean and Grosjean,[29] and the OH yield of 0.35, with the assumption that part of the RO_2 radical (labeled 1°-β-hydroxy-RO_2) that is coproduced with OH makes formaldehyde; thus the direct formaldehyde yield was reduced by 0.18. The portion of the carbon that does not make carbonyls was then assumed to make the C_1 and C_2 Criegee intermediates; in a proportion of 45:55 (inferred from the apparent branching observed in the carbonyls; more formaldehyde is produced than acetaldehyde). The C_2 is assumed to make only OH (0.25) and 1°-β-hydroxy-RO_2, and the C_1 is assumed to make 0.1OH + HO_2 + CO, with the remainder generating (CO_2 + H_2), (CO + H_2O), and (2H + CO_2) in proportions of 0.2:0.7:0.1. CO_2, H_2, and H_2O are ignored since they are not reactive. [c] Reference 30. [d] The rate constants and products of the self-reactions and RO_2−HO_2 reactions are from Lightfoot et al.[31] and Jenkin and Hayman.[32] The rate constants are the geometric average of the self-reaction rate constants, and the products are the arithmetic averages. [e] Reference 25. [f] Approximated (this work). [g] Measured (this work). [h] Approximated from ref 28: products were derived from existing data for TMB and assumed to be the same for *m*-xylene. [i] Approximated from structure−activity relationships[33] or analogous compounds (for aromatics). [j] Indicates that, although a particular compound is specified, this product is not the exact compound that is thought to form, but has a very similar reactivity with respect to reaction with the OH radical. ROOH = organic hydroperoxide, RO_2 = organic peroxy radical, RACID = organic acid, RALD = aldehyde. Production of CO and CO_2 is ignored.

are small. Ozone−alkene reactions generate aldehydes in almost unit yield; since these react rapidly with OH they must be included. O_3 (which is added in aliquots) is specified as a first-order source term with a rate constant consistent with the alkene

consumption rate observed in each experiment (the sensitivity to this approximation is investigated below). The experiments were stopped after 55−75% of the alkene was consumed because both the chemistry and the chromatograms become increasingly complex as the experiment progresses. This is a compromise between a good signal and increasing side reactions and products.

As part of a related study[25] we have measured the rate constants for the reactions to which the OH yield is most sensitive: the OH reaction with tracers TMB, XYL, and DBE. We have also measured the rate constants for O_3 reactions with TMB and XYL, as well as wall loss rates for O_3, TMB, XYL, and DBE (wall loss rates in a chamber are completely negligible for hydrocarbons with less than about six carbon atoms. Table 1 summarizes the initial conditions and OH yields calculated with the model.

Systematic Uncertainties. The largest source of uncertainty inherent in this small-ratio relative-rate method is that associated with the OH-tracer rate constants. Any uncertainty in these values is translated directly into the OH yield uncertainty. We believe that these values are known to better than ±12% (95% confidence interval; for a detailed discussion, see ref 25). In contrast, since the alkene is in excess, uncertainty in its rate coefficient has a smaller affect on the calculated OH yield. For example, a 10% difference in the rate constant for OH + alkene reaction results in a less than 1% difference in the calculated OH yield, as long as T/A is small.

The OH yield derived from this method is quite insensitive to uncertainty in T_0/A_0, except when the ratio is large (e.g., $\gtrsim$0.3, depending on the alkene/tracer combination; see Figure 1). For example, for a small ratio propene experiment, a 30% change in the ratio shifts the calculated OH yield by 3−5%. Since the maximum uncertainty in the initial ratios is ±6%, this source of error is negligible.

The yield of aldehydes from the ozone−alkene reaction is another potential source of systematic uncertainty. Since aldehydes react rapidly with OH radicals and build up to high concentrations toward the end of the experiment, they can compete for a significant portion of the OH radicals. For aldehyde yields that have been measured in the presence of OH scavengers, ±25% is a reasonable estimate for their uncertainty (see notes in Table 2). For example, for propene experiments with reasonably small T_0/A_0, adjusting the aldehyde yields by ±25% shifts the OH yield prediction by 2−7%, in the same direction as the change in the aldehyde yield. Many of the expected products are organic peroxides, since the RO_2-HO_2 reactions are fairly rapid, and HO_2 is generated both from the O_3−alkene reactions and from most RO_2-RO_2 reactions. Organic peroxides react fairly rapidly with OH, and both the yields and the OH reaction rate constants for these compounds are uncertain, and introduce an additional uncertainty that is probably equivalent to that arising from the aldehyde uncertainty.

There are several smaller sources of uncertainty that are common to most (if not all) methods of measuring OH formation yields. Increasing the tracer wall loss rate by a factor of 2 in the propene experiments (the uncertainty for our wall loss rates are ±60%[25]) decreases the predicted OH yield by 4−6%. The slow reaction of tracers with O_3 has a negligible affect for all alkenes except those that both react slowly with O_3 and have small OH yields. OH radicals can arise from the reactions of O_3 with HO_2 or H atoms ((R3)−(R4)), producing an uncertain quantity of OH. Nearly all H atoms react with O_2 to produce HO_2, and most HO_2 reacts with the RO_2 radicals that form in the OH and O_3 reactions with hydrocarbons. For example, doubling the HO_2 yield (which may be a realistic assessment of its uncertainty) results in a 2−3% decrease in the OH yield. Since O_3 is added in 8−15 concentrated aliquots, the O_3 concentration is also variable. The concentration of O_3 in the aliquot itself can be as high as 200−2000 ppm, but this is rapidly diluted as it mixes into the reaction chamber. The model uses an O_3 concentration that represents the *average* behavior of the O_3 in the chamber; it starts at zero and increases to several ppm, depending on the alkene concentration. A 200-fold increase in the (model) ozone concentration has a negligible affect on the OH yield (i.e., <0.5%).

The systematic uncertainties for small-ratio propene experiments combine to about ±13−15%. For large ratio experiments, the systematic uncertainties will be larger, $\gtrsim$50%.

Random Uncertainties. There are several sources of random uncertainty in this type of measurement. Any error in the relative concentration measurement caused by coeluting peaks translates directly into an error in the slope, which affects the predicted OH yield depending on the conditions of the experiment. For propene experiments at small ratios, a 5% error translates into about a 7% effect on the OH yield (this can be derived from (E7)). An error in an initial concentration is amplified in the resulting slopes by a factor of 2−10 or more (see also (E7)); the smaller the amount of tracer consumed in an experiment, the larger the amplification factor. This particular set of experiments was prone to an uncertainty in the initial concentrations (due to incomplete mixing before the initial addition of O_3). Those with more than a 1% uncertainty were not included here. These two sources of error account for the observed scatter in these experiments of about ±12% (2σ).

Combining systematic and random uncertainties, an overall uncertainty of ±15−25% can be expected for alkenes that react with O_3 at moderate rates, provided small T_0/A_0 ratios and fast reacting tracers such as TMB are used. For ethene and butadiene the best uncertainty is ±25−35%. Uncertainties are higher (~±50% or more) for large T_0/A_0 ratio experiments.

Experimental Results

Propene. To verify this method, we have carried out several types of experiments using the propene−O_3 reaction as the OH source. Initial ratios (T_0/A_0) were varied from 0.02 to 6.2. Three tracers were used, alone or in pairs. In the experiments described here we have added pairs of tracers for two reasons. First, each experiment provides two data sets from which to calculate the OH yield. Second, the tracer pair concentrations may be plotted according to the equation:

$$\frac{k_{T_1}}{k_{T_2}} = \frac{\ln([T_1]_0/[T_1]_t)}{\ln([T_2]_0/[T_2]_t)} \qquad \text{(E12)}$$

where k_{T_i} and T_i are the OH reaction rate constants and concentrations, respectively, for the ith tracer. The resulting slope may be compared with that predicted by reaction of tracers with OH (see also ref 6). Since XYL and DBE elute close to one another on our column, we use TMB and either XYL or DBE. Ultrapure nitrogen was used in place of air in one experiment. The initial concentrations, T_0/A_0, OH yields, and special conditions are summarized in Table 1. Figure 2 shows the effect of the T_0/A_0 on tracer consumption and the calculated OH yield for three experiments that used TMB as tracer. Figure 3 shows the results from two representative small-ratio experiments, PDT-77 and PDT-719, both of which used a pair of tracers (TMB and DBE). Figure 4 shows the results for PXT-

117, which was carried out in ultrahigh purity nitrogen. The T_0/A_0 ratios for these experiments are in the region where the slopes should be close to their maximum values (Figure 1). Figures 3 and 4 clearly demonstrate that the amount of tracer consumed is directly proportional to its OH reaction rate constant; about twice as much TMB reacts as DBE, and 2.5 times as much TMB relative to XYL in each case (see also (E12) and ref 6). The experiment shown in Figure 4 was not oxygen free; the chamber was rinsed twice with N_2, and then filled with N_2, but some O_2 was added with the O_3. The O_2 concentration was not measured but is expected to be at least a factor of 10 lower than in air. The OH yields calculated for this experiment are equal to the average for the experiments carried out in air, indicating that O_2 probably does not significantly affect the OH formation mechanism and that the O_2 mediated reactions of RO_2 and RO radicals, which generate some HO_2 and potentially OH, do not significantly affect the results.

The average OH yield for 9 experiments (13 observations) is 0.346 ± 0.045 (2σ). As discussed above, this uncertainty arises from random error; an additional systematic error of ±15% must also be included; this results in an overall uncertainty of ±19%, or 0.35 ± 0.07. Across the set of experiments, there is no observable trend in the OH yield with respect to T_0/A_0 (i.e., OH yields do not show an apparent increase or decrease as the initial ratio becomes larger). Likewise the 30-fold variation in the initial concentrations of propene and tracers (from 3 to 93 and 0.22 to 9 ppm respectively; Table 1) has no effect on the calculated OH yield.

Ethene. Initial concentrations and results for five experiments with initial $T_0/A_0 < 0.2$ are summarized in Table 1, and the data and model calculations for three experiments are shown in Figure 5. Ethene data were analyzed using the numerical model that was a version of that shown in Table 2 tailored to ethene. The products assumed for the ozone reaction with ethene were:

$$\text{ethene} + O_3 \rightarrow \text{HCHO} + 0.13H_2 + 0.44\text{CO} + 0.37H_2\text{COO} + 0.12HO_2 + 0.18\text{OH} \quad \text{(R11)}$$

As for propene, the slopes are larger for smaller initial ratios, and the relative decay of tracers XYL and DBE are approximately half that of the tracer TMB. Experiment ET-625 contained a small quantity of propene; this was included in the model. Experiment ET-317 was carried out in an FTIR long-path cell. The average OH yield from the model calculations is 0.18 ± 0.03 (2σ, 7 observations). Taking into consideration the possible systematic uncertainties discussed above results in a final value for the formation yield of OH from the ozone−ethene reaction of 0.18 ± 0.06.

Discussion

Our OH yield for the propene−O_3 reaction of 0.35 ± 0.07 is in excellent agreement with the measurement of Atkinson and Aschmann[5] of 0.33 (+0.17, −0.11) but it is significantly larger than the values of Gutbrod et al.[17] and Horie and Moortgat[26] of 0.18 and 0.17, respectively. Our value for ethene of 0.18 ± 0.06 is in reasonable agreement with the measurement of Atkinson and Aschmann[5] of 0.12 (+0.06, −0.04), and is again significantly higher than the value obtained by Gutbrod et al.[15] of 0.08 (no uncertainty was specified). The only other available measurement for ethene was made at 5.5 Torr; using a direct method, Donahue et al.[7] found an OH yield of (0.43, +0.21, −0.15), clearly higher than our value. The comparability of this measurement is unclear, however, since the pressure dependence of the OH formation channel has yet to be established. We have made preliminary measurements indicating that OH yields may increase at lower pressures for some alkenes (Fenske and Paulson, unpublished work). We have measured OH yields for several additional alkenes and find that our results are generally in reasonable agreement (within the uncertainties, but some are significantly higher or lower) with the values reported by Atkinson and co-workers (e.g., refs 23 and 27). Except in the case of isoprene, our values are larger than those of Gutbrod et al.[15,17] and Horie and Moortgat[26] by a factor of 2−3. The reasons for these discrepancies are still to be determined.

Conclusions

The small-ratio relative-rate technique provides a reasonably straightforward method to derive OH yields with uncertainties in the ±15−30% range from ozone-alkene reactions. Fast reacting tracers are required, and aldehyde formation from the alkene reaction with O_3 must be reasonably well characterized to achieve these error limits. We have applied this technique to the O_3 reactions with propene and ethene and find OH formation yields of 0.35 ± 0.07 and 0.18 ± 0.06, respectively. The OH yield can be derived by solving the set of ordinary differential equations that describe the chemistry of the experiment, or in some cases, by using an analytical solution that accounts for only the three or four most important reactions.

Acknowledgment. Acknowledgment is made to the donors of the Petroleum Research Fund, administered by the ACS, for partial support of this research, and the National Science Foundation under ATM-9629577. The authors thank Dana Uehara, Gerardo Loera, Jaime Prescilla, and Grazyna Orzechowska for assistance with chamber experiments, Drs. John Orlando and Geoffrey Tyndall for kind assistance with the FTIR apparatus used for experiment ET-317, Jon S. Jacobs for providing a clean sample of TMB on short notice in Boulder, and Prof. G. Barney Ellison for helpful discussions.

References and Notes

(1) Hatakeyama, S.; Akimoto, H. *Res. Chem. Intermed.* **1994**, *20*, 503−24.
(2) Niki, H.; Maker, P. D.; Savage, C. M.; Breitenbach, L. P.; Hurley, M. D. *J. Am. Chem. Soc.* **1987**, *91*, 941−6.
(3) Atkinson, R.; Aschmann, S. M.; Arey, J.; Shorees, B. *J. Geophys. Res.* **1992**, *97*, 6065−73.
(4) Paulson, S. E.; Flagan, R. C.; Seinfeld, J. H. *Int. J. Chem. Kinet.* **1992**, *24*, 79−102.
(5) Atkinson, R.; Aschmann, S. *Environ. Sci. Technol.* **1993**, *27*, 1357−63.
(6) Paulson, S. E.; Sen, A. D.; Liu, P.; Fenske, J. D.; Fox, M. J. *Geophys. Res. Lett.* **1997**, *24*, 3193−6.
(7) Donahue, N. M.; Kroll, J. H.; Anderson, J. G.; Demerjian, K. L. *Geophys. Res. Lett.* **1998**, *25*, 59−62.
(8) Marston, G.; McGill, C. D.; Rickard, A. R. *Geophys. Res. Lett.* **1998**, *25*, 2177−80.
(9) Paulson, S. E.; Orlando, J. J. *Geophys. Res. Lett.* **1996**, *23*, 3727−30.
(10) Hu, J.; Stedman, D. H. *Environ. Sci. Technol.* **1995**, *29*, 1655−9.
(11) Horie, O.; Neeb, P.; Moortgat, G. K. *Int. J. Chem. Kinet.* **1994**, *26*, 1075−94.
(12) Paulson, S. E.; Seinfeld, J. H. *Environ. Sci. Technol.* **1992**, *26*, 1165−1173.
(13) Curley, M.; Treacy, J.; Sidebottom, H. *Physio-Chemical Behaviour of Atmospheric Pollutants*; European Commission: Varese, Italy, 1993; pp 220−225.
(14) Chew, A. A.; Atkinson, R. *J. Geophys. Res.* **1996**, *101*, 28649−53.
(15) Gutbrod, R.; Meyer, S.; Rahman, M. M.; Schindler, R. N. *Int. J. Chem. Kinet.* **1997**, *29*, 717−23.
(16) Gutbrod, R.; Schindler, R. N.; Kraka, E.; Cremer, D. *Chem. Phys. Lett.* **1996**, *252*, 221−9.

(17) Gutbrod, R.; Kraka, E.; Schindler, R. N.; Cremer, D. *J. Am. Chem. Soc.* **1997**, *119*, 7330−42.
(18) Atkinson, R.; Tuazon, E. C.; Aschmann, S. M. *Environ. Sci. Technol.* **1995**, *29*, 1860−6.
(19) Paulson, S. E.; Flagan, R. C.; Seinfeld, J. H. *Int. J. Chem. Kinet.* **1992**, *24*, 103−25.
(20) Schafer, C.; Horie, O.; Crowley, J. N.; Moortgat, G. K. *Geophys. Res. Lett.* **1997**, *24*, 1611−4.
(21) Finlayson-Pitts, B. J.; Pitts, J. *Atmospheric Chemistry: Fundamentals and Experimental Techniques*; Wiley-Interscience: New York, 1986.
(22) Martinez, R. I.; Herron, J. T.; Huie, R. E. *J. Am. Chem. Soc.* **1981**, *103*, 3807−20.
(23) Paulson, S.; Chung, M.; Sen, A.; Orzechowska, G. *J. Geophys. Res.* **1998**, *103*, 25533−9.
(24) Carter, W.; Atkinson, R. *Calif. Air Resources Board* 1988.
(25) Kramp, F.; Paulson, S. E. *J. Phys. Chem.* **1998**, *102*, 2685−90.
(26) Horie, O.; Moortgat, G. K. *Atmos. Environ.* **1991**, *25A*, 1881−96.
(27) Kramp, F.; Paulson, S. E. manuscript in preparation.
(28) Atkinson, R. *J. Phys. Chem. Ref. Data* 1994, Monograph No. 2, 1−216.
(29) Grosjean, E.; Grosjean, D. *Environ. Sci. Technol.* **1997**, *31*, 2421−7.
(30) Lightfoot, P. D.; Cox, R. A.; Crowley, J. N.; Destriau, M.; Hayman, G. D.; Jenkin, M. E.; Moortgat, G. K.; Zabel, F. *Atmos. Environ.* **1992**, *26A*, 1805−1961.
(31) Jenkin, M. E.; Hayman, G. D. *J. Chem. Soc., Faraday Trans.* **1995**, *91*, 1911−22.
(32) DeMore,W. B.; Sander, S. P.; Golden, D. M.; Hampson, R. F.; Kurylo, M. J.; Howard, C. J.; Ravishankara, A. R.; Kolb, C. E.; Molina, M. J. Jet Propulsion Laboratory Publication 97-4, 1997.
(33) Kwok, E. S. C.; Atkinson, R. *Atmos. Environ.* **1995**, *29*, 1685−95.
(34) Moortgat, G. K.; Cox, R. A.; Schuster, G.; Burrows, J. P.; Tyndall, J. *J. Chem. Soc., Faraday Trans. 2* **1989**, *85*, 809−29.
(35) Tuazon, E. C.; Aschmann, S. M.; Arey, J.; Atkinson, R. *Environ. Sci. Technol.* **1997**, *31*, 3004−9.